JOURNAL OF CATALYSIS **120,** 314–324 (1989)

The Surface Chemistry of Isolated and Aggregated Silica-Bound Rhodium Complexes

K. C. CANNON AND J. M. WHITE

Department of Chemistry, University of Texas at Austin, Austin, Texas 78712

Received February 23, 1989; revised July 12, 1989

The chemisorption activity of silica-bound molecular Rh complexes has been studied using Fourier transform infrared, temperature-programmed desorption, and X-ray photoelectron spectroscopy on samples treated variously with CO, NO, and H_2. Beginning with a μ-oxo rhodium carbonyl species, treatment with NO leads to no (bis)nitrosyl rhodium complexes but to a mixture of an oxygen adduct and a nitrite/nitrate complex. Treatment of the latter with CO does not form isocyanate; treatment of it with H_2 leads to an aggregated Rh complex and an unidentified complex, probably involving nitrogen and derived from the nitrate/nitrite complex. Treatment of the aggregated complex with NO and CO leads to some isocyanate on the Rh but none on the support. High-temperature treatment under vacuum leads to irreversible sintering after which the Rh behaves like conventional Rh metal particles with respect to formation of isocyanate on both the metal and the support upon exposure to NO and CO. We conclude that isocyanate formation depends strongly on the form of the Rh.

INTRODUCTION

In a previous publication (*1*) we reported the transformations which take place when the silica-attached rhodium μ-oxo carbonyl complex $([SiO]Rh(CO)_2)_2$ **1** reacts with nitric oxide. Complex **1** had been characterized at the molecular level previously (*2, 3*), and, therefore, provided valuable information concerning the reactivity of an "ultradispersed" rhodium sample toward nitric oxide reduction by carbon monoxide.

The transformations we observed upon reaction with NO and subsequent treatment with CO differed significantly from reactions involving metallic Rh particles (*4–10*); by IR analysis we observed neither rhodium bis(nitrosyl) nor isocyanate complex formation from **1** below 250°C, and reduction of NO at temperatures as high as 400°C yielded less than 2% rhodium isocyanate complex. We attribute these differences to the molecular nature of the Rh throughout our experiments.

Reaction of the rhodium μ-oxo carbonyl complex **1** with NO at temperatures between 100 and 250°C resulted in the formation of the rhodium oxygen adduct $([SiO]RhO_2)_2$ **2** (80%) and a rhodium nitrate/nitrite species **3** (20%) (*1*) (Scheme 1). Reaction of the mixture of **2** and **3** with CO regenerated complex **1** from **2;** the rhodium nitrate/nitrite complex **3** did not react with CO. Further reaction with NO produced no additional nitrate/nitrite complex. At 400°C in the presence of NO, complex **3** decomposed; a similar observation was reported by Arai and Tominaga (*5*).

In this paper, we report on aggregation of molecular Rh complexes and their activity for the formation of isocyanate species during reaction of NO with CO. Fourier transform infrared spectroscopy (FTIR), temperature-programmed desorption (TPD), and X-ray photoelectron spectroscopy (XPS) are used to characterize adsorbed species and the Rh. Conversion of isolated molecular silica-attached rhodium complexes to aggregates of undetermined nuclearity is achieved by treatment with H_2 (*2*). In addition to the aggregation of the rhodium oxygen adduct **2,** reaction with H_2 resulted in the conversion of the rhodium nitrate/nitrite species **3** to an undetermined

0021-9517/89 $3.00

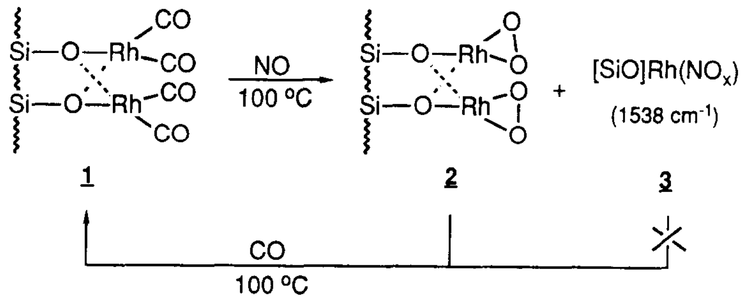

SCHEME 1

surface complex identified by an IR absorption at 1986.2 cm^{-1}. With these aggregates, rhodium isocyanate complexes formed during subsequent exposure to NO and CO.

EXPERIMENTAL

Experiments were performed in two ultrahigh vacuum (UHV) systems, one focusing on XPS and the other on FTIR and TPD. Both allowed *in situ* treatment with reactive gases.

X-ray photoelectron spectroscopy. Photoemission experiments were performed with a VG ESCALAB Mark I spectrometer system (Mg$K\alpha$ X-ray source). Binding energies (BE) were determined within an uncertainty of ± 0.1 eV. The system included a preparation chamber equipped with sample heating and gas-handling lines. During dosing, the pressure in the preparation chamber was monitored by a MSK baratron (Type 170M-6C).

Infrared spectroscopy and temperature-programmed desorption. This UHV system is partitioned by a gate valve into two chambers. The first is equipped with a double-pass cylindrical mirror analyzer (CMA) and a UTI 100C quadrupole mass spectrometer. The second chamber, which serves as the preparation chamber, has two CaF_2 windows (Harshaw) positioned to transmit the FTIR beam through the chamber to a mercury cadmium telluride (MCT) detector. Infrared spectra were recorded on a Mattson Cygnus 100 with a resolution of 4 cm^{-1}. In several cases, FTIR spectra were repetitively taken (4 per minute) during dosing or temperature programming. Spectra of the silica-supported complexes were collected in transmission. External optics were continuously purged with dry nitrogen. Dosing pressures in the preparation chamber were monitored by a MKS baratron capacitance manometer. A Varian variable leak valve connected the two chambers for the mass spectrometric analysis of the gas mixtures in the preparation chamber.

Temperature-programmed desorption was performed with the UTI 100C quadrupole mass spectrometer. The temperature ramp rate was typically 5.3°C s^{-1}. TPD was performed with the sample in the reaction chamber (as opposed to line-of-sight) to enable concomitant use of FTIR spectroscopy.

Substrate preparation. Silica samples were pressed into a highly transparent tantalum mesh (50 mesh, CPI, Inc.) which had been previously spot-welded to two tantalum wires. These wires were then connected to a pair of copper heating leads. The sample was resistively heated through the tantalum by an external power supply and was conductively cooled by contact with a liquid nitrogen reservoir above the sample. Temperatures were measured with a chromel–alumel thermocouple spot-welded to the tantalum mesh.

Preparation of ([SiO]Rh(CO)$_2$)$_2$ ***1.*** The preparation and characterization of the starting material, rhodium μ-oxo carbonyl complex **1,** has been described in detail previously (*1*). A 25-mg sample of the silica-attached rhodium bis(allyl) complex (1.80 wt% Rh/SiO_2) *in vacuo* was exposed to 30 Torr of CO at ambient temperature for 2 h. Evacuation of CO yielded the rhodium μ-oxo carbonyl complex **1**. In order to remove adsorbed water from the sample due to handling in air, initially formed **1** was heated gradually to 200°C under 1×10^{-6} Torr of O_2. Retreatment of the sample with CO (30 Torr, 100°C) resulted in **1** (Fig. 1a). ν_{CO} = 2103.3 (sh), 2093.4 (s), and 2035.7 (s) cm^{-1}.

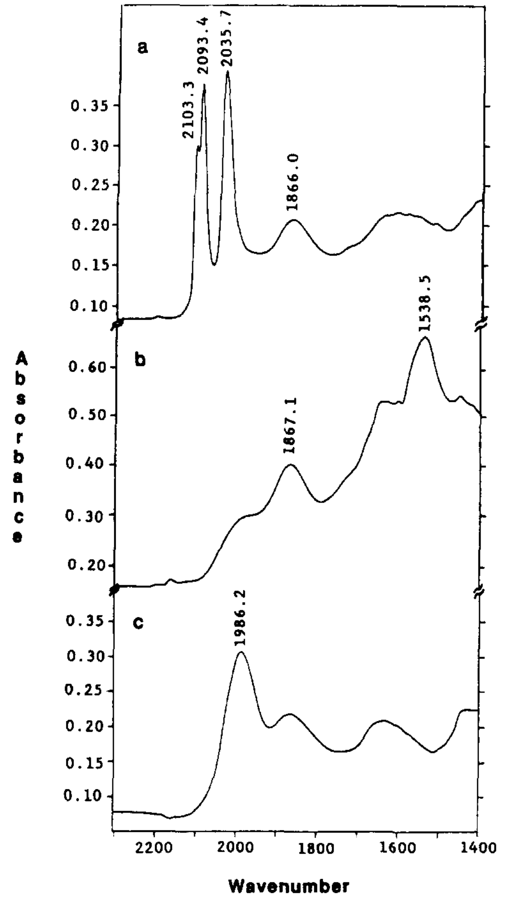

FIG. 1. IR spectra of the reaction of rhodium μ-oxo carbonyl complex **1** with NO and subsequent reaction with H_2: (a) rhodium μ-oxo carbonyl complex $([SiO]Rh(CO)_2)_2$ **1**; (b) mixture of rhodium oxygen adduct $([SiO]RhO_2)_2$ **2** and rhodium nitrate/nitrite complex $[SiO]Rh(NO_x)$ **3** generated from the μ-oxo carbonyl complex (30 Torr NO, 100°C, 1 h); (c) sample after treatment with H_2 (25 Torr H_2, 200°C, 2 h).

A ^{13}CO-enriched rhodium μ-oxo carbonyl complex (>95% enrichment) was prepared by exposing **1** to 20 Torr of ^{13}CO at 90°C for 1.5 h. $\nu^{13}CO$ = 2054.4 (sh), 2042.4 (s), and 1988.2 (s) cm^{-1}.

3. RESULTS AND DISCUSSION

3.1 Preparation of $([SiO]RhO_2)_2$ *2 and* $[SiO]Rh(NO_x)$ *3*

Reaction of the silica-attached rhodium μ-oxo carbonyl complex, $([SiO]Rh(CO)_2)_2$ **1**, with NO at 100°C resulted (Scheme 1) in a mixture of a rhodium oxygen adduct $([SiO]RhO_2)_2$ **2** and a rhodium nitrate/nitrite complex **3** (*1*). The transformations on rhodium were monitored by FTIR spectroscopy. Figure 1a is the IR spectrum of the rhodium carbonyl complex **1**. The 1866–1867 cm^{-1} absorption in Fig. 1 is due to a Si–O combination band originating from the silica support. Reaction with NO (30 Torr, 100°C, 1 h) resulted in the rapid loss of carbonyl absorptions (≅90% in the first minute of exposure) and the appearance of a new absorption at 1538.5 cm^{-1} attributed to formation of the rhodium nitrate/nitrite complex **3** (Fig. 1b).

Previously, complex **3** had only been characterized by IR (*1, 5*). Using TPD and IR spectroscopies simultaneously, we can now unambiguously assign the 1538.5 cm^{-1} absorption as a nitrogen oxide species. TPD spectroscopy (Fig. 2) performed on the mixture of **2** and **3** produced a single peak, T_p = 323°C, due to the desorption of NO (m/e = 30); a smaller single peak, T_p = 407°C, was also produced for m/e = 44 (CO_2 and/or N_2O). CO_2 desorption could result from the reaction of residual carbonyl ligands which were present in this particular sample. The disappearance of the 1538 cm^{-1} absorption corresponded well to the desorption of NO (Fig. 2). No peaks were observed for m/e = 46; neither NO_2 nor any higher nitrogen oxide was desorbed directly. This suggested that upon thermolysis, the nitrate/nitrite ligand decomposed to NO, but the fate of the remainder of the

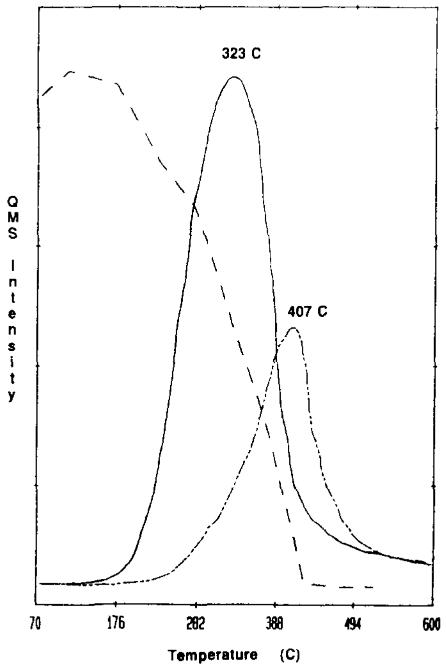

FIG. 2. TPD and FTIR of the mixture of rhodium oxygen adduct ($[SiO]RhO_2)_2$ **2** and rhodium nitrate/nitrite complex $[SiO]Rh(NO_x)$ **3** generated from the μ-oxo carbonyl complex **1** (30 Torr NO, 100°C, 1 h). The dashed curve is the integrated area of the 1538.5 cm^{-1} absorption characteristic of the nitrate/nitrite complex, which diminishes to zero by the conclusion of TPD. The solid curve is $m/e = 30$ (NO), and the dot-dashed curve is $m/e = 44$ TPD.

oxygen atoms is unclear. No desorption of O_2 ($m/e = 32$) was detected. Preparation in the XPS system followed by evacuation gave $Rh(3d_{5/2})$ at 310.1 eV BE.

The rhodium nitrate/nitrite complex **3** does not react with CO at temperatures as high as 200°C, while the rhodium oxygen adduct **2** reacted with 30 Torr CO at 100°C to regenerate the initial carbonyl complex **1.** IR analysis demonstrated that further reaction with NO does not produce more **3.** Therefore, dividing the integrated area of carbonyl complex which is regenerated from **2** by the integrated area of the initial carbonyl complex determined the yield of **2.** The remainder of the surface rhodium complexes was assumed to be **3.** In our previous investigation, this technique determined that the reaction of the rhodium μ-oxo carbonyl complex **1** with NO (30 Torr, 100°C, 1 h) produced 80% **2** and 20% **3** (*1*). In this investigation, identical reaction conditions yielded 86% **2** and 14% **3.**

The 20% yield of rhodium nitrate/nitrite complex was obtained from samples which were 1.97 wt% Rh/SiO_2. In our present investigation, however, 1.80 wt% Rh/SiO_2 was used. This suggests that increasing the amount of $Rh(C_3H_5)_3$ deposited on SiO_2 may result in new surface complexes; a similar correlation has been observed for oxide-attached rhodium carbonyl complexes, although at significantly higher loadings (*11*). These new surface complexes may differ in subtle structural or geometric properties and may be susceptible to nitrate/nitrite formation. Further investigation is necessary to establish the validity of the relationship between rhodium nitrate/nitrite formation and the amount of rhodium complex deposited on silica.

3.2 Reaction of Complexes 2 and 3 with H_2

Reaction of the mixture of rhodium oxygen adduct **2** and rhodium nitrate/nitrite complex **3** with H_2 was monitored by IR. The sample was initially treated with 25 Torr of H_2 at room temperature; the temperature of the sample was then increased in increments of 25°C. Between 175 and 200°C, reaction of the nitrate/nitrite complex **3** with H_2 was noted by the gradual loss of intensity of the 1538.5-cm^{-1} absorption, and the appearance of a new absorption at 1986.2 cm^{-1} (Fig. 1c). No additional growth in this absorption was detected after two additional hours at 200°C under 200 Torr of H_2. After this treatment, the binding energy of $Rh(3d_{5/2})$ XPS was 308.8 eV. Figure 3 demonstrates the direct relationship between the reaction of the nitrate/nitrite complex **3** with H_2 and the appearance of the 1986.2-cm^{-1} absorption by comparing the integrated areas of the respective absorption bands.

The synthesis of this complex was repeated with a ^{13}C-enriched rhodium μ-oxo

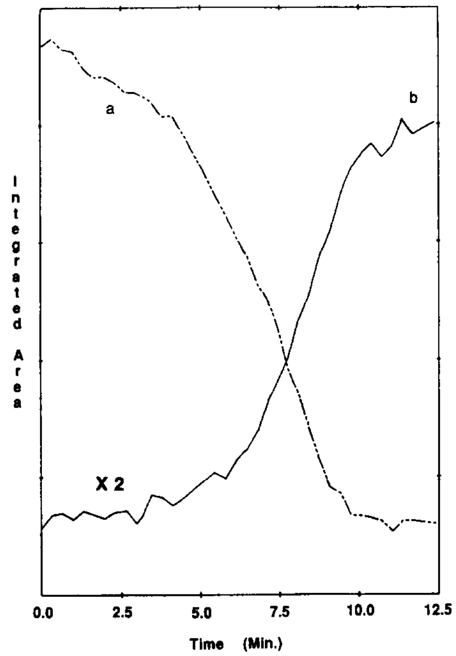

FIG. 3. Time dependence of: (a) the 1538.5-cm^{-1} intensity (the rhodium nitrate/nitrite complex [SiO]Rh(NO_x) **3**) and (b) the 1986.2-cm^{-1} intensity during exposure to H_2 (25 Torr, 175–200°C).

carbonyl complex **1** (>95% enrichment, $\nu^{13}CO$ = 2054.4 (sh), 2042.4 (s), and 1988.2 (s) cm^{-1}) and D_2 under identical reaction conditions. No change was observed by IR, indicating that the 1986.2-cm^{-1} absorption was *not* due to the presence of a rhodium carbonyl or hydride species. When the mixture of complexes **2** and **3** was exposed to D_2, H–D exchange between the atmosphere and residual hydroxyl groups of the silica support (*12*) was effected at 100°C prior to formation of the new species, thereby eliminating the possibility that hydride formation via reaction with residual surface hydroxyl groups was responsible for the absorption at 1986.2-cm^{-1}. The frequency of this absorption is also outside the range commonly observed for linearly coordinated nitrosyl ligands. TPD and IR spectroscopies used simultaneously on the sample synthesized from the ^{13}C-enriched carbonyl complex **1** and D_2 confirmed that the unidentified absorption was not due to rhodium hydride, carbonyl, or nitrosyl complexes; desorption of D_2 (m/e = 4) and ^{13}CO (m/e = 29) was insignificant. Although some desorption was observed for m/e = 28 (N_2?) and m/e = 44 (N_2O?), the results were ambiguous because the amounts were barely distinguishable from background. No desorption of NO (m/e = 30), O_2 (m/e = 32), and NO_2 (m/e = 46) was observed. At the conclusion of TPD (600°C), the surface complex had completely decomposed as measured by FTIR. While an identification of the species responsible for the 1986.2-cm^{-1} band has not been made, several possibilities have been eliminated. Ideas about its origin are discussed below.

3.3 The Effect of H_2 Silica-Attached Rhodium Complexes

To determine whether the reaction with H_2 resulted in a change in surface coordination to the rhodium metal center, the H_2-treated sample exhibiting the 1986.2-cm^{-1} absorption was reacted with CO (30 Torr, 100°C, 1.5 h) and monitored by IR. The rapid disappearance of the 1986.2-cm^{-1} absorption was observed (during the first minute of exposure), and a mixture of rhodium carbonyl complexes resulted (Fig. 4) In addition to the μ-oxo carbonyl **1** (regenerated from rhodium oxygen adduct **2**), the formation of an aggregate rhodium carbonyl complex(es) **5** of undetermined nuclearity was indicated by a new terminal carbonyl absorption at 2065.2 cm^{-1} and a bridging carbonyl absorption at 1864.0 cm^{-1}. Although the absorption of the bridging carbonyl ligand occurs in the same frequency range as that of the silica combination band (1867 cm^{-1}), the presence of the carbonyl absorption was ascertained by comparing the relative intensity of this band to the absorption at 1621 cm^{-1}.

Reaction of the H_2-treated sample with CO also produced a rhodium isocyanate complex identified by a weak, broad absorption at 2195.6 cm^{-1}. This absorption indicated that the isocyanate ligand was coordinated to the rhodium metal center;

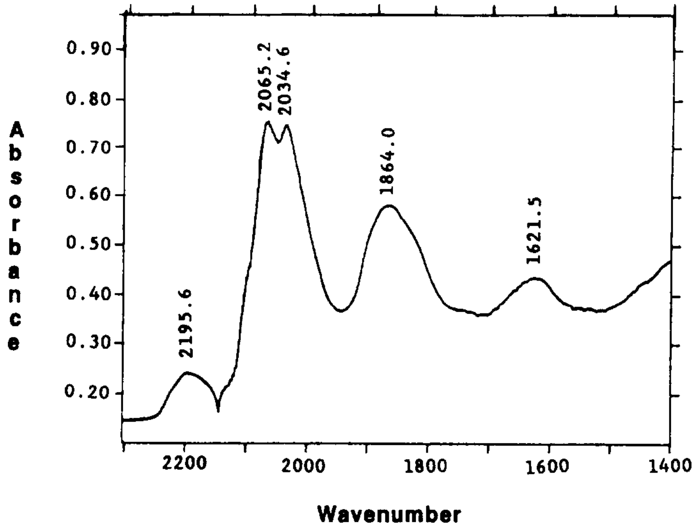

FIG. 4. IR spectrum of the carbonyl complexes resulting from the reaction of the H_2-treated sample (Fig. 1c) with CO (30 Torr, 100°C, 1.5 h). The absorption at 2034.6 cm^{-1} is due to the presence of the μ-oxo carbonyl complex **1**. Absorptions at 2065.2 cm^{-1} (terminal CO) and 1864.0 cm^{-1} (bridging CO) represent the formation of aggregate rhodium carbonyl complex **5** (nuclearity unknown). The absorption at 2195.6 cm^{-1} is characteristic of the rhodium isocyanate complex.

transfer of isocyanate ligand to the silica support, characterized by an absorption peak at 2300 cm^{-1} (*13*), was not observed.

Synthesis of the isocyanate complex requires the presence of a nitrogen-containing species formed during the reaction of rhodium nitrate/nitrite complex **3** and H_2. We speculate that this nitrogen-containing species was responsible for the undetermined structure giving rise to the 1986.2-cm^{-1} absorption in the IR of the H_2-treated sample (Fig. 1c). Although the value of this IR absorption falls within the range reported for rhodium dinitrogen adducts (*14*), a recent publication by Wang and Yates (*15*) discourages such an assignment. The absorption of N_2 on rhodium-impregnated alumina was investigated, and the formation of a rhodium nitrogen adduct at <-33 C was identified by an IR absorption at 2257 cm^{-1}. TPD/IR analysis of the 1986-cm^{-1} absorption determined desorption and/or decomposition to take place at temperatures exceeding 350 C. It is very unlikely that molecular nitrogen would bond so strongly to a rhodium metal center.

Formation of the aggregate rhodium carbonyl complex **5** (for a representation, see Scheme 2) may occur via two routes. The first route (Eq. 1) would involve hydrogenation of silica-attached rhodium complexes **2** and **3** to yield rhodium crystallites. Subsequent reaction with CO is known to generate **5** (*16*):

$$\underset{\mathbf{3}\ (x\,=\,2,\,3)}{[\mathrm{SiO}]\mathrm{Rh}(\mathrm{NO}_x)} + \mathrm{H}_2 \rightarrow [\mathrm{Rh}^{\mathrm{o}}]_n + [\mathrm{SiOH}]$$

$$+\ \mathrm{CO} \rightarrow \underset{\mathbf{5}}{([\mathrm{SiO}]\mathrm{Rh}(\mathrm{CO})_2)_n}. \quad (1)$$

However, XPS data (Fig. 5) does not support the existence of rhodium crystallites in the H_2-treated sample. Previous work shows that Rh crystallites generated by thermolysis of silica-attached rhodium complexes exhibit a binding energy of 307.3 eV (Rh $3d_{5/2}$) (*17*). In our work, the Rh $3d_{5/2}$ binding energy of the H_2-treated sample was 308.8 eV, which falls outside the range reported for Rh metal (*18*). Although it is possible that crystallites may exist in quantities below the limits of detection, the in-

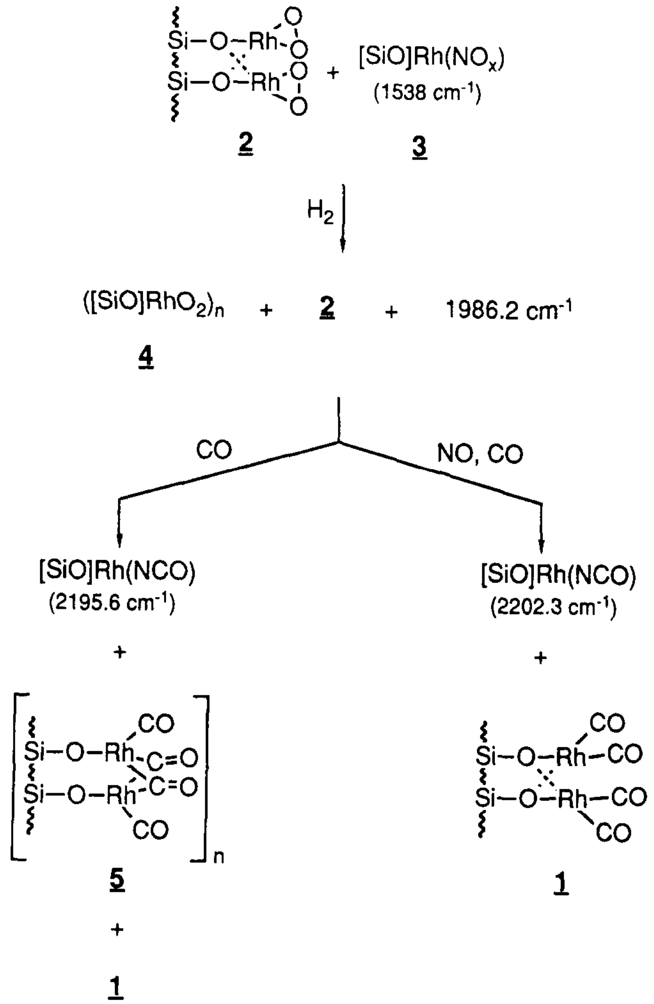

SCHEME 2

tensity of the aggregate carbonyl FTIR absorptions suggests that if the existence of crystallites was primarily responsible for the formation of **5**, then their concentration would certainly lie within XPS detection limits.

The second, and favored, route for forming the aggregate rhodium carbonyl complex **5** involves the H_2-promoted migration of silica-attached rhodium complexes without a formal reduction in the Rh oxidation state. In this model, for example, rhodium oxygen adduct **2** would migrate in the presence of H_2 and form adduct **4**, which converts to **5** upon reaction with CO:

$$\underset{\mathbf{2}}{([\mathrm{SiO}]\mathrm{RhO_2})_2} + \mathrm{H_2} \rightarrow \underset{\mathbf{4}}{([\mathrm{SiO}]\mathrm{RhO_2})_n}$$

$$+ \mathrm{CO} \rightarrow \underset{\mathbf{5}}{([\mathrm{SiO}]\mathrm{Rh(CO)_2})_n}. \quad (2)$$

This process is not surprising, as the H_2-promoted migration of silica-attached organorhodium complexes have been previously documented (*2, 11*).

XPS was utilized to investigate the effect of H_2 on complex **2** (Fig. 5). The Rh $3d_{5/2}$ binding energy for **2** was 310.0 eV (Fig. 5a). The formal oxidation state of the rhodium metal center of the oxygen adduct is Rh^{+3}.

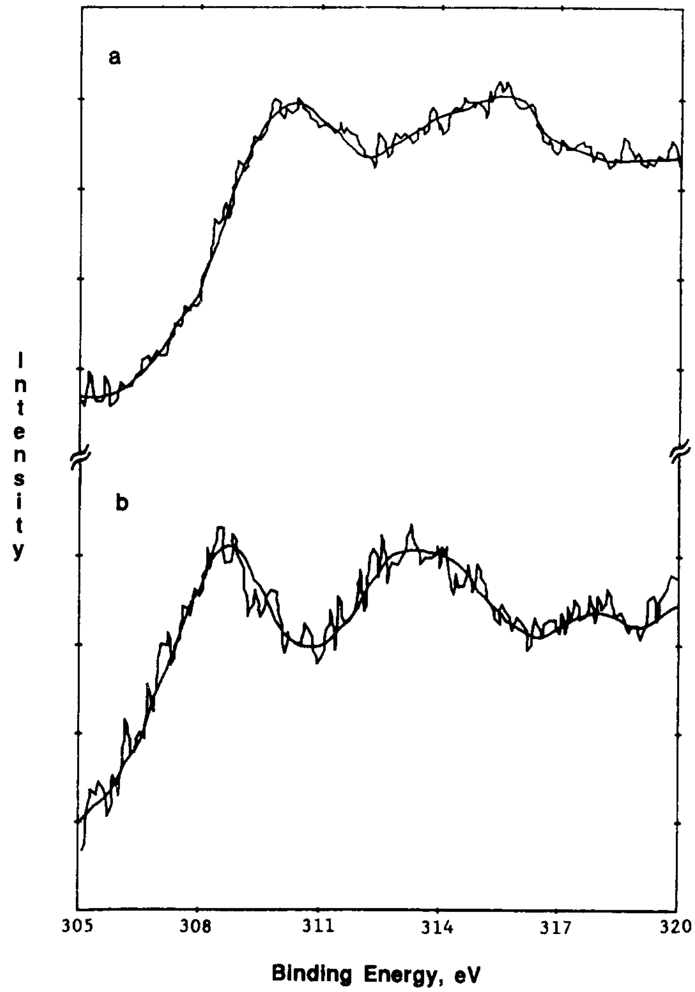

FIG. 5. XPS spectra of Rh 3d: (a) sample of a mixture of rhodium oxygen adduct ($([SiO]RhO_2)_2$) **2** and rhodium nitrate/nitrite complex $[SiO]Rh(NO_x)$ **3** generated from the μ-oxo carbonyl complex **1** before reaction with H_2. $3d_{5/2}$ BE = 310.0 eV; (b) sample after reaction with H_2 (25 Torr, 200°C, 2 h). $3d_{5/2}$ BE = 308.8 eV.

The Rh $3d_{5/2}$ binding energy for the rhodium nitrate/nitrite complex **3** could not be resolved (*1*). After reaction with H_2 (25 Torr, 200°C, 2 h), the binding energy of the Rh $3d_{5/2}$ electron decreased to 308.8 eV (Fig. 5b). The formal oxidation state of rhodium in this sample is ambiguous as it falls within the range of both Rh^{+1} (307.6–309.6 eV) and Rh^{+3} (308.8–311.3 eV) complexes (*19*). The observed decrease in binding energy does not necessarily imply a reduction in the formal oxidation state of rhodium. Conversion of dimeric complex **2** to an aggregate with three or more rhodium metal centers would result in a decrease in the Rh $3d_{5/2}$ binding energy even if no formal reduction in oxidation state has occurred (*20*), and we have determined by IR spectroscopy that aggregation has indeed taken place (see above). Frederick, Apai, and Rhodin (*21*) demonstrated this effect in an XPS study of rhodium carbonyls on alumina; aggregated carbonyl complexes exhibited a binding energy 0.7 eV lower than that of nonaggregated complexes. Unfortunately, we cannot distinguish the contribution of aggregation and formal reduction to the 1.2-eV BE decrease.

3.4 Reaction of the H_2-Treated Sample with NO and CO

Reaction of the H_2-treated sample with NO (30 Torr, 100°C, 1 h) was analyzed by IR spectroscopy (Fig. 6). The H_2-treated sample, Fig. 6a, exhibited an absorption at 1986.2 cm^{-1}. Upon addition of NO, rapid loss of this absorption was observed. Completion of the reaction yielded a sample which contained an absorption at 1534.2 cm^{-1} (w, br), which we associate with a rhodium nitrate/nitrite surface species (Fig. 6b). However, this absorption disappeared when the sample was reacted with CO (see below), and therefore cannot be due to complex **3**. New absorptions (Fig. 6b) at 1742.5 cm^{-1} (w, br) and 1605.7 cm^{-1} (w) were also observed; although these may be due to the presence of rhodium nitrosyl complexes, they are not equivalent to those found on metal particles (*4–10*).

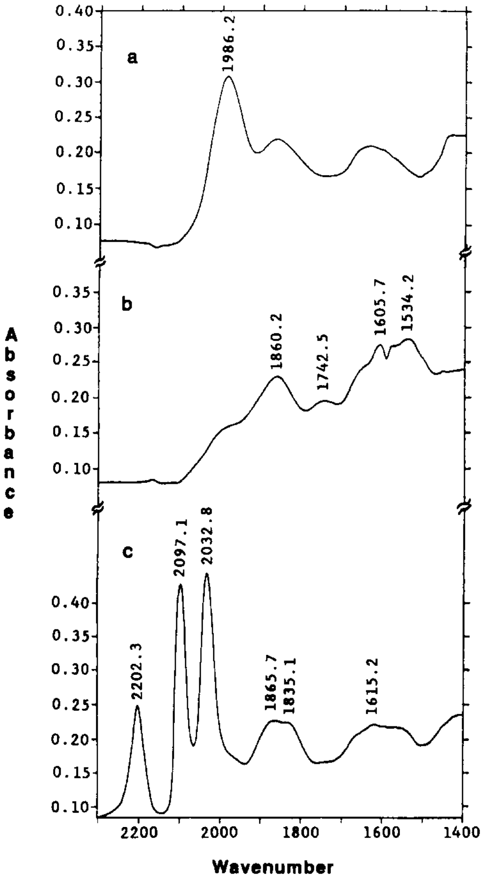

FIG. 6. IR spectra of the reaction of the H_2-treated sample, Fig. 1c, with NO, and subsequent reaction with CO: (a) mixture of rhodium oxygen adduct $([SiO]RhO_2)_2$ **2** and rhodium nitrate/nitrite complex $[SiO]Rh(NO_x)$ **3** which has been reacted with H_2 (25 Torr, 200°C, 2 h); (b) H_2-treated sample after reaction with NO (30 Torr, 100°C, 1 h); (c) mixture of rhodium carbonyl complex (2097.1 cm^{-1} and 2032.8 cm^{-1}) and isocyanate complex (2202.3 cm^{-1}) formed upon reaction with CO (30 Torr, 100°C, 1.5 h).

Treatment of the sample with CO (30 Torr, 100°C, 1.5 h) produced an absorption at 2202.3 cm^{-1} (m) characteristic of the rhodium isocyanate complex (Fig. 6c). There was no absorption at 2300 cm^{-1}, indicating that no isocyanate was on the support (*13*). The small shoulder at 1835.1 cm^{-1} (bridging carbonyl ligands) indicates the formation of an aggregate rhodium carbonyl complex; the low frequency of the bridging carbonyl absorption and lack of the terminal carbonyl stretch suggest this aggregate was not complex **5**. A rhodium surface complex containing terminal isocyanate ligands and bridging carbonyl ligands would account for these observations.

Thus, by reacting a mixture which was 86% rhodium oxygen adduct **2** and 14% rhodium nitrate/nitrite complex **3** with H_2 (25 Torr, 200°C, 2 h), rhodium aggregates formed and resulted in the production of rhodium isocyanate complexes, upon reaction with NO and CO at 100°C. In our previous investigation (*1*), isocyanate complex formation was not observed with samples not pretreated with H_2 but otherwise identical conditions; at reaction temperatures of 400°C, only 2% conversion to the isocyanate complex was realized. Using the integrated areas of the carbonyl absorptions, the regenerated sample consisted of 77% carbonyl complex and 23% isocyanate complex. At face value, these numbers suggest that the isocyanate complex formation cannot be attributed solely to the initial presence of rhodium nitrate/nitrite complex **3** and its subsequent reaction with H_2. However, these calculations must be used cautiously since the rhodium *m*-oxo carbonyl complex **1** was not exclusively regenerated (Fig. 6c). Further investigation is necessary to determine the contribution, if any, of rhodium oxygen adduct aggregation in isocyanate complex formation.

3.5 Extended High-Temperature Treatment of Complexes

Over the course of this paper we have stressed the differences between supported Rh, prepared by our method, and that prepared by conventional wet impregnation methods (molecular Rh vs Rh crystallites). To assure ourselves that we could obtain data consistent with literature on Rh crystallites, we examined the results of long-term heating of adsorbed complexes. In one experiment, after the TPD of Fig. 2, the sample was held at 600°C under vacuum for 2 h.

Obvious changes occurred. First, the sample turned black, indicating formation of small metallic Rh particles. Second, after cooling, exposure to CO showed none of the original complex; the spectrum was dominated by terminal- and bridge-bonded CO as expected for metal crystallites. Third, exposure to NO gave high intensity for the bis(nitrosyl) complex. Fourth, following the NO dose with a CO dose led to large amounts of isocyanate both on Rh and on the support. Finally, these changes were irreversible; none of the cyclic transformations indicated in Schemes 1 and 2 could be achieved.

These results are in excellent agreement with the literature on supported Rh particles and, as such, provide an internal consistency check on the comparisons we make here between the structure/reactivity of molecular complexes and metal particles.

4. SUMMARY

The reaction sequences performed in this investigation are summarized in Scheme 2. Treatment of a mixture of rhodium oxygen adduct **2** and rhodium nitrate/nitrite complex **3** with H_2 (25 Torr, 200°C, 2 h) resulted in the formation of a new surface complex characterized by an IR absorption at 1986.2 cm^{-1}. The appearance of this new absorption corresponded to the consumption of the nitrate/nitrite complex. The identity of this new surface complex is unknown, but TPD and IR analysis of isotopically enriched samples show that it is not a carbonyl, a hydride, or a nitrosyl complex. Based on connections with isocyanate formation, it probably contains nitrogen.

Treatment of the H_2-treated sample with CO (30 Torr, 100°C, 1.5 h) shows that, in addition to reaction with **3,** H_2 facilitated some migration and aggregation of **2;** this was evidenced by the intensity of the carbonyl absorptions at 2065.2 cm^{-1} (terminal CO) and 1864.0 cm^{-1} (bridging CO). These absorptions are assigned to complex **5,** an aggregate rhodium carbonyl complex of undetermined nuclearity. An alternate pathway for the formation of **5** (via crystallites) was not substantiated by XPS. Although reaction of complexes **2** and **3** with H_2 resulted in a 1.2-eV decrease in the Rh $3d_{5/2}$ binding energy (from 310.0 to 308.8 eV), there was no evidence for the formation of rhodium crystallites. Formation of a rhodium isocyanate complex was also identified by IR analysis. The absorption at 2195.6 cm^{-1} indicated that the isocyanate group was coordinated to the rhodium metal center. IR analysis exhibited no evidence of migration of the isocyanate ligand to the silica support.

Reaction of the H_2-treated sample with NO (30 Torr, 100°C, 1 h) and subsequent reaction with CO (30 Torr, 100°C, 1.5 h) resulted in the formation of rhodium μ-oxo carbonyl complex **1** and the rhodium isocyanate complex (2202.3 cm^{-1}).

These observations point to a structure/reactivity correlation for the reduction of NO by CO. In our previous investigation (*1*), as here, molecular rhodium complexes, covalently attached to an oxide support, exhibited chemical transformations significantly different from rhodium samples prepared by wet impregnation/high-temperature reduction with H_2. We believe that the difference in chemistry is due to the molecular nature of our complexes versus the particulate nature of the latter. Upon conversion of dimeric, silica-attached complexes to aggregates by H_2-promoted migration of the rhodium metal centers, a change in reactivity occurs; rhodium isocyanate complex formation, previously observed in insignificant yields at temperatures as high as 400°C, occurs readily at 100°C. Thus, the formation of rhodium isocyanate complexes is directly linked to the presence of rhodium aggregate complexes. The importance of this observation is realized when the catalytic applications of rhodium for NO reduction in automative exhausts are considered. Isocyanate complex formation is an undesirable side reaction (*22*).

The transformations which take place on our H_2-treated (aggregated) sample still differed significantly from samples investigated previously. For example, we observed no transfer of the isocyanate ligand from the rhodium metal center to the oxide support, probably due to the absence of crystallites which are proposed to facilitate spillover (*13*). Similar reactivity was achieved only after thermal decomposition (600°C, 2 h) of the silica-attached complexes.

ACKNOWLEDGMENTS

This research was supported in part by the U.S. Department of Energy, Office of Basic Energy Sciences. We thank Jeff Cook for assistance with the XPS measurements.

REFERENCES

1. Cannon, K. C., Jo, S. K., and White, J. M., *J. Amer. Chem. Soc.* **111,** 5064 (1989).
2. McNulty, G. S., Cannon, K., and Schwartz, J., *J. Inorg. Chem.* **25,** 2919 (1986).
3. Schwartz, J., and Fischer, H. E., in preparation.
4. Hyde, E. A., Reedham, R., and Rochester, C. H., *J. Chem. Soc. Faraday Trans. 1* **80,** 531 (1988).
5. Arai, H., and Tominaga, H., *J. Catal.* **43,** 131 (1976).
6. Solymosi, F., and Sàrkany, J., *Appl. Surf. Sci.* **3,** 68 (1979).
7. Solymosi, F., Bànsàgi, T., and Novàk, E., *J. Catal.* **112,** 183 (1988).
8. Iizuka, T., and Lunsford, J. H., *J. Mol. Cat.* **8,** 391 (1980).
9. Liang, J., Wang, H. P., and Spicer, L. D., *J. Phys. Chem.* **89,** 5840 (1985).
10. Rives-Arnau, V., and Munuera, G., *Appl. Surf. Sci.* **6,** 122 (1980).
11. Cannon, K. C., Ph.D. thesis, Princeton Univ., 1987.
12. Ward, M. D., and Schwartz, J., *Organometallics* **1,** 1030 (1982).
13. Hecker, W. C., and Bell, A. T., *J. Catal.* **85,** 389 (1984).
14. Werner, H., Wolf, J., and Schubert, U., *Chem. Ber.* **116**(b), 2848–2854 (1983).
15. Wang, H. P., and Yates, J. T., Jr., *J. Phys. Chem.* **88**(5), 852–856 (1984).
16. Basu, P., Panayotov, D., and Yates, J. T., Jr., *J. Amer. Chem. Soc.* **110,** 2074 (1988).
17. Schwartz, J., *Acc. Chem. Res.* **18,** 302 (1985).
18. Huzinga, T., van't Blick, H. F. J., Vis, R., and Prins, J. C., *Surf. Sci.* **135,** 580 (1983).
19. Andersson, SL. T., Watters, K. L., and Howe, R. F., *J. Catal.* **69,** 212 (1981).
20. Parmigiani, F., Bagus, P. S., Nelin, C. J., and Kay, E., *J. Electron Spectrosc. Relat. Phenom.* **36,** 257 (1985).
21. Frederick, B. G., Apai, G., and Rhodin, T. N., *J. Amer. Chem. Soc.* **109,** 4797 (1987).
22. Unland, M. T., *J. Catal.* **31,** 459 (1973).